



CHORUS

This is the accepted manuscript made available via CHORUS. The article has been published as:

Theory of Carbomorph Cycles

Oleg E. Shklyaev, Eric Mockensturm, and Vincent H. Crespi

Phys. Rev. Lett. **110**, 156803 — Published 9 April 2013

DOI: [10.1103/PhysRevLett.110.156803](https://doi.org/10.1103/PhysRevLett.110.156803)

Theory of Carbomorph Cycles

Oleg E. Shklyae, Eric Mockensturm
Department of Mechanical and Nuclear Engineering

Vincent H. Crespi
*Department of Physics and Materials Research Institute,
The Pennsylvania State University, University Park, PA, 16802-6300, USA*
(Dated: February 11, 2013)

We present a theory of a reversibly deforming sp^2 -carbon based system controlled by competing strain, surface, and electrostatic energies, a *carbomorph*. For example, external forces (such as electrostatic, chemical, interfacial) could convert a bistable carbon nanotube between the collapsed and inflated states. Such a system could operate as a voltage-controlled constant-force spring, a charge-controlled harmonic spring, or an electromechanical engine or generator (with linear stroke up to few microns) driven across a propagating quasi-one-dimensional structural phase transition.

PACS numbers: 61.48.De, 85.85+j, 85.35.Kt, 64.70.Nd

Most macroscale electro-mechanical motors are rotary and use mechanical linkages to create linear motion. At smaller scales linkages are harder to construct; Nature has instead developed direct linear motors to power cellular processes at the micro- and nanoscale. Although several nanoscale rotary motors have been proposed¹⁻³, artificial linear nanomotors capable of long, micron-scale power strokes are lacking. Rotaxane motors⁴ are limited to displacements of a few nanometers, and other linear actuators generally cannot produce displacements comparable to size of the device. Here we describe the theory of a large-displacement linear motor composed of an electrically actuated variable-shape bistable carbon nanotube. This one-dimensional working body undergoes changes in shape that are easily coupled to external forces. The nanotube's bistability makes possible a two-state "digital" motor that generates constant-force work. By modulating the relative stability of the two states, diverse electromechanical working cycles can be designed.

Single-walled nanotubes of appropriate diameters have locally stable inflated and collapsed states⁵⁻¹⁰ as shown in Fig. 1. Strain energy favors high-symmetry structures of uniform curvature and surface energy favors low-symmetry structures with opposing surfaces in contact. Excess charge on the tube wall favors the inflated state, thereby enabling electromechanical switching^{11,12}. The high and low symmetry states are separated by an activation barrier, even if the system is tuned so that they are degenerate. However, boundary conditions that clamp opposite ends open and closed enforce a transition region between the states and hence enable facile conversion between them. The imposition of these boundary conditions is a challenge for the practical realization of a device. A tube could be held open by a rigid endcap that forms during synthesis, either due to a metal catalyst particle on the end or the closure of the sp^2 framework through incorporation of pentagonal rings; the second case apparently occurs in Figure 5 of reference¹³, which shows a tapering of the tube cross-section and pronounced deformation of graphenic lattice planes where the collapse front collides with a rigid tube endcap. A tube could be

held closed by mechanical compression or bending¹⁴. In general, we call a variable-shape sp^2 carbon-based system where the competition between strain and surface energies is moderated by an externally controllable stimulus (voltage, temperature, etc.) a *carbomorph*.

Consider a metallic single-walled carbon nanotube of length L containing a net charge qL which induces potential V on the tube relative to infinity. Take the tube diameter large enough that it prefers to be collapsed at zero voltage and clamp one end of it in the inflated state, the other in the collapsed state. If the shape of the transition region between inflation and collapse is independent of its location along the tube axis and the cross-sectional shape of the collapsed region does not depend significantly on voltage across the range of device operation, then the tube configuration can be described by a single degree of freedom: the fraction $0 \leq \ell \leq 1$ of the tube which is inflated. The mechanical energies and capacitances per unit length are constant within each inflated/collapsed section, and the total energy decomposes into independent mechanical¹⁵ and electrostatic contributions.

A tube rapidly equilibrates to a charge $q = CV$ with the usual RC time constant. Then on a much slower timescale the tube equilibrates to the proper mixture of collapsed and inflated states for the given charge, with a slow change in C . A mesoscale analogue of the Born-Oppenheimer approximation applies: the system maintains near-instantaneous *charge* equilibrium on an electronic timescale while evolving slowly towards *shape* equilibrium on a mechanical timescale¹⁷. This distinction ensures that the state of the tube can be described by a single voltage V relative to ground on the mechanical timescale. The voltage, charge per unit length, and inflated fraction are related by a simple equation of state:

$$V = \frac{q}{C_-(1-\ell) + C_\circ\ell}. \quad (1)$$

C_- and C_\circ are the capacitances per unit length of the inflated and collapsed states. Any two of q , V , and ℓ can be independently varied while holding the third fixed to define arms of a nano-electromechanical cycle. Making

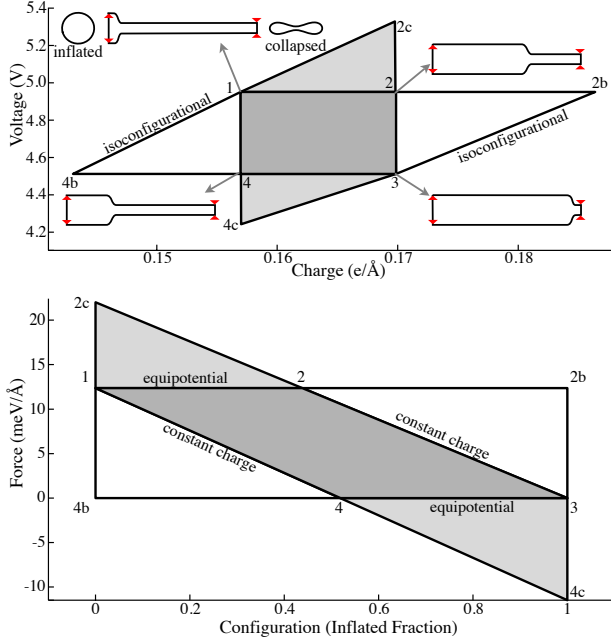


FIG. 1: Electromechanical cycles of a (40,40) nanotube carbomorph in charge-voltage ($q-V$) and shape-force ($\ell-F$) coordinates. White, light and dark areas show isoconfigurational/equipotential (ℓV), constant-charge/isoconfigurational ($q\ell$), and constant-charge/equipotential (qV) cycles, respectively. These cycles are designed so that the extrema correspond to fully inflated and collapsed states ($\ell_1 = 0$, $\ell_3 = 1$) with a lower voltage at which collapse and inflation are degenerate ($V_3 = V_d$). The upper operating voltage V_1 is chosen to maximize the net work (i.e. area enclosed) of the qV cycle. Elongated shapes are schematic representations of the tube viewed on its side, indicating its state of (partial) collapse. On either side of the upper-left tube are representations of the tubes' cross-section.

an analogy to ideal-gas thermodynamics, equipotential ($|_V$), constant-charge ($|_q$) and isoconfigurational ($|_\ell$) processes correspond to isothermal, adiabatic and isochoric processes. We will first analyze these three component processes and then combine them into operational cycles.

The energy budget of a tube connected to a charge reservoir must account for both the capacitor self-energy $q^2/2C$ and the work performed by the battery (qV for charge q supplied at voltage V). The isoconfigurational process performs no mechanical work and operates simply as a constant-shape capacitor operating on the fast RC time scale. During an equipotential process the carbomorph acts as a shape-changing capacitor which charges slowly at fixed voltage. Half of the work qV done by the battery (i.e. $CV^2/2$) goes towards charging the carbomorph's instantaneous shape, while the remainder goes towards a combination of mechanical work performed on the environment and mechanical dissipation. In general, mechanical work is favored when an external load guides the shape change to occur slowly, as described below.

The total energy per unit length is

$$E|_V = [(E_o - C_o V^2/2)\ell + (E_- - C_- V^2/2)(1 - \ell)], \quad (2)$$

E_- and E_o are the mechanical energies per unit length of the collapsed and inflated states. We define a degeneracy voltage $V_d = \sqrt{2 \frac{E_- - E_o}{C_- - C_o}}$ such that the system prefers the collapsed state ($\ell = 0$) when $V < V_d$ and the inflated state ($\ell = 1$) when $V > V_d$. During an equipotential process the transition region exerts a constant force $\frac{\partial E}{\partial \ell}|_V = (C_o - C_-)(V^2 - V_d^2)/2$ as it approaches equilibrium. An equipotential carbomorph operates as a voltage-controlled constant-force spring which can couple to cargo (solid, liquid or gas¹¹) inside or outside the tube.

During the constant-charge process (i.e. when disconnected from the battery), the electrostatic energy per unit length is simply $q^2/2C$. A fixed charge distributes between the collapsed and inflated regions as $q = q_o \ell + q_-(1 - \ell)$, such that both ℓ and V evolve to an equilibrium that minimizes

$$E|_q = E_o \ell + E_-(1 - \ell) + qV/2, \quad (3)$$

with V given by the equation of state (1). Two important threshold charges determine the equilibrium shape: the charges necessary in the collapsed (q_1) and inflated (q_2) states to generate a voltage V_d . Below q_1 (above q_2) the equilibrium is $\ell = 0$ ($\ell = 1$). For $q_1 \leq q \leq q_2$ the equilibrium is a mixed collapsed/inflated state with configuration $\ell^* \in [0, 1]$ determined by the charge q . The linearized restoring force, $\frac{\partial E}{\partial \ell}|_q = 2(\ell - \ell^*)(C_- - C_o)(E_- - E_o)/q$, about this state is harmonic, so that motion of the transition region can sense external force, pressure or temperature, revealing them through changes in ℓ .

Pairwise combinations of these three processes, plus external forces on the moving transition region, yield three distinct cycles which we call qV , ℓV and $q\ell$ as shown in Fig. 1. The qV cycle (1,2,3,4) has a theoretical maximum efficiency of 100% in converting electrical to mechanical work (or vice versa) but requires precise timing during operation and a precisely controlled coupling to external force. The ℓV cycle (1,2b,3,4b) can be driven by a simple electrical signal, but is 100% efficient only in the limit of zero work performed. The $q\ell$ cycle (1,2c,3,4c) requires a simple mechanical stimulus, but is 100% efficient only in the limiting case of a vanishingly short isoconfigurational arm (and again, zero net work performed).

First consider the qV cycle, which contains two equipotential and two constant-charge processes as shown by the dark shading in Fig. 1. The cycle is defined by V_i , q_i , ℓ_i ($i = 1..4$) as related by the state equation (1). Consider a cycle that is bounded below by the voltage V_d at which inflated and collapsed states are degenerate. For highest efficiency, consider a full-stroke cycle, i.e. $\ell_1 = 0$ and $\ell_3 = 1$. Since the electromechanical coupling derives from the difference in capacitances of the inflated and collapsed states, we can express many physical quantities in terms of $\gamma = C_o/C_-$. Further defining a reduced voltage $\nu = V_1/V_d$, with $V_{3,4} = V_d$, we set the high-voltage arm at $V_{1,2} = [(1 + \gamma)/2]V_d$ to maximize the electrical work $W_{qV} = C_- V_3^2 (\nu - 1)(\gamma \nu - 1)$ performed in the cycle.

When operated clockwise, the qV cycle $1 \rightarrow 2 \rightarrow 3 \rightarrow 4$ is an electrically powered actuator. Along arm $1 \rightarrow 2$

the tube draws charge from a high-voltage battery and thereby inflates from ℓ_1 to ℓ_2 , the capacitance and charge growing linearly as the tube performs constant-force work on the surroundings. Along the constant-charge path $2 \rightarrow 3$ the carbomorph continues to inflate (ℓ_2 is not an equilibrium shape for constant charge), performing additional mechanical work until reaching ℓ_3 . A low-voltage battery with $V_3 = V_d$ is then connected to facilitate the path $3 \rightarrow 4$. This return stroke occurs at *zero* net force; charge leaves, the capacitance shrinks, and the carbomorph collapses from ℓ_3 to ℓ_4 . Precisely at $V_3 = V_d$, the time required for the return stroke $3 \rightarrow 4$ diverges and in the absence of assistance, the carbomorph configuration is determined by fluctuations of temperature, pressure, voltage, etc. Voltages above V_d require an external force along $3 \rightarrow 4$; those below are spontaneous and can perform additional work on the environment. Finally, the path $4 \rightarrow 1$ requires external mechanical work to force further tube collapse, decrease the capacitance and increase the voltage at constant charge, thereby completing the cycle. This cycle occurs without any isoconfigurational charging of the capacitor: the 50% wastage of input power in isoconfigurational capacitor charging from a constant-voltage battery is thereby avoided.

Overall device efficiency is a complex matter, with multiple contributions depending on the precise device implementation. We focus first on the efficiencies within the simple single-degree-of-freedom model and later extend the discussion to include atomic-scale dissipation. We write the device efficiency as $\eta|_{qV}$ for motor operation (electrical to mechanical conversion) and $\xi|_{qV}$ for generator operation (mechanical to electrical conversion), where the subscripts indicate what is held constant in successive arms of the cycle. η is the ratio of the mechanical work around the cycle to the change in the electric energy. ξ is the ratio of the change in the electric energy around the cycle to the mechanical work. Due to the inherently dissipative isoconfigurational process, $\xi \neq 1/\eta$ for $q\ell$ and ℓV cycles. The engine and generator efficiencies of an ideal qV cycle are both one. The unusual charging dynamics of a variable-shape capacitor make this possible. The charge/discharge of the variable-shape capacitor during the qV loop requires no intrinsic resistive loss in the limit of low series resistance. Of course, in real systems various nonidealities will reduce the efficiency, but the practical operating efficiency could conceivably approach the established high efficiencies of e.g. macroscopic DC motors. Note, however that the qV cycle must be driven by precisely timed and shaped voltages and forces.

The ℓV cycle (1,2b,3,4b) consists of two equipotential and two isoconfigurational processes. It requires simple step changes in voltage without precise timing, and we choose $V_3 = V_d$ and $V_1 = V_{\max}$ to facilitate comparison with the qV cycle. The tube inflates from ℓ_1 to ℓ_{2b} at constant voltage V_1 , gaining charge $q_{2b} - q_1$ and performing constant-force work. When the voltage is reduced to V_3 , the charge rapidly (i.e. isoconfigurationally) adjusts at a fixed $\ell_3 = \ell_{2b}$. Along the equipotential path $3 \rightarrow 4b$ ($V_{4b} = V_3$), the inflated fraction shrinks

to zero and the carbomorph loses charge. Isoconfigurational charging from $4b$ to 1 completes the cycle, thus converting a simple electrical signal into constant-force work $W_{\ell V} = \frac{1}{2}C_-V_3^2(\gamma - 1)(\nu^2 - 1)$ when $\ell_1 = 0$ and $\ell_{2b} = 1$. Choosing $V_1 \geq V_d$ and $V_3 \leq V_d$ would produce a cycle powered entirely electrically with no external source of mechanical work required.

The ℓV cycle suffers inescapable resistive losses during isoconfigurational charge/discharge: independent of the size of the resistance in series with the battery, half of the work supplied by the battery is lost (if the voltage source operates at a piecewise constant voltage, as for standard batteries). For the ℓV cycle $W_{in} = C_-V_3^2(\gamma\nu - 1)(\nu - 1)$, $W_{out} = W_{\ell V}$ such that

$$\eta|_{\ell V} = \frac{1}{2} \left(1 - \frac{\gamma - \nu}{1 - \gamma\nu} \right) \leq 1. \quad (4)$$

The efficiency $\eta|_{\ell V}$ is zero when the inflated and collapsed states have the same capacitance (i.e. $\gamma = 1$). It is $\frac{1}{2}$ when $\gamma = \nu$ ($q_3 = q_1$). $\eta|_{\ell V} = 1$ when the inherently dissipative isoconfigurational processes become negligible (i.e. $\nu = 1$ or $V_3 = V_1$), but in this case no work is performed around the cycle. Reversing the cycle to $4b \rightarrow 3 \rightarrow 2b \rightarrow 1$ yields the generator efficiency

$$\xi|_{\ell V} = \frac{2(\gamma - \nu)}{(\gamma - 1)(\nu + 1)} \leq 1 \quad (5)$$

which is zero when the isoconfigurational processes are negligible ($\gamma = \nu$) and one when the voltage swing is zero ($\nu = 1$). The ℓV cycle has a simple voltage signal.

The engine and generator efficiencies have a simple graphical representation, depicted in Fig. 2. In the middle panel, η is the ratio of the area of the dark grey inner parallelogram – the mechanical work – to the area of the light grey outer rectangle – the change in electric energy. In the bottom panel, ξ is the ratio of dark grey rectangle to the outer light grey parallelogram. For the ideal qV cycle, both areas are rectangles so the efficiency is one.

The $q\ell$ cycle (1,2c,3,4c) consists of isoconfigurational and constant-charge arms shown by the light grey shading in Fig. 1. We choose the same voltage swing ($V_1 \leftrightarrow V_3$) as for the qV cycle. In engine mode this cycle performs mechanical work $W_{q\ell} = C_-V_3^2(\gamma^2 - \nu^2)(\gamma - 1)/2\gamma$ along constant-charge strokes $2c \rightarrow 3$ and $4c \rightarrow 1$. The efficiency

$$\eta|_{q\ell} = \frac{1}{2} \left(1 - \gamma \frac{\nu - 1}{\nu - \gamma^2} \right) \leq 1 \quad (6)$$

is zero when $\gamma = 1$, $\frac{1}{2}$ when $\nu = 1$, and one when $\gamma = \nu$. In generator mode ($4c \rightarrow 3 \rightarrow 2c \rightarrow 1$), the surroundings perform mechanical work on the carbomorph and pump charge from a low- to high-voltage battery. Along $4c \rightarrow 3$, the low-voltage battery (at V_3) charges the inflated tube to q_3 isoconfigurationally. Next, the tube is detached from the battery and mechanically collapsed by external forces along a constant-charge path, $3 \rightarrow 2c$. The tube then discharges into the high-voltage battery V_{1b} along an isoconfigurational path $2c \rightarrow 1$, replenishing the charge reservoir. When the external force driving

collapse is removed, the tube spontaneously inflates along the constant-charge path $1 \rightarrow 4c$ until it reaches an equilibrium configuration at a potential V_d (at the intermediate point 4 in the cycle). To continue inflation, external force must be applied. As the tube inflates, the capacitance increases and voltage decreases until it reaches V_{4c} . Mechanical work is performed along the constant-charge paths $3 \rightarrow 2c$ and $1 \rightarrow 4c$. The change in the electric energy around the cycle, is $(V_1 - V_3)(C_o V_3 - C_- V_1)$. Therefore the generator efficiency is

$$\xi|_{q\ell} = \frac{2\gamma(\nu - 1)}{(\gamma - 1)(\nu + \gamma)} \leq 1. \quad (7)$$

Again, the efficiency is zero when the operational voltage swing is zero ($\xi|_{q\ell} = 0$ when $\nu = 1$) and one when the loop shrinks in a manner that the isoconfigurational processes disappear ($\xi|_{q\ell} = 1$ when $\gamma = \nu$). The $q\ell$ cycle has a particularly simple force signal.

At the atomic scale, the system generates phonons during front propagation. We have performed molecular dynamics simulations for propagating collapse fronts coupled to external loads, monitoring the amount of energy that persists as kinetic energy in the moving front, is extracted as useful work by the load, or dissipates as thermal vibrations. Supplementary materials¹⁸ provide details for a $1 \mu\text{m}$ long (45,45) tube. Larger external loads decrease the front speed and thus reduce dissipation, so efficiency increases at lower operating frequencies. Under modest load and GHz frequencies, a large fraction ($\sim 50\%$) of the initial potential energy of inflation can be captured in organized mechanical motions, i.e. the kinetic energy of the front and mechanical work of the load. The small size of the device limits heating to a few Kelvins. Free oscillations of a collapsing carbomorph front against one end of the device decay at a rate consistent with the efficiency estimates. A large fraction of the ideal efficiency η can be attained, even after accounting for atomistic mechanical dissipation.

A carbomorph exploits a displacive structural transition with a very large (nanometer-scale) atomic displacement in a system with every constituent atom exposed. These features give it new ways of coupling to its environment that are not available to traditional phase-change materials (e.g. shape-memory alloys), such as charge-based actuation which is faster and more easily integrated than thermal actuation. Unlike other quasi-one-dimensional systems that also exploit internal phase boundaries for switching, such as ‘‘racetrack’’ magnetic memories in ferromagnetic nanowires, the two states of the carbomorph – inflated and collapsed – are not related by a symmetry transformation. For example, the elastic moduli, electric conductivity¹⁹, and vibrational entropies of the inflated and collapsed carbomorphs can

differ substantially, facilitating new device modalities. In addition, since charge is a conserved quantity whereas magnetization is not, a fixed-charge mode is readily accessed (whereas a magnetic system in equilibrium is limited to fixed-field operation). Some of this physics can be extended to other types of shape changing capaci-

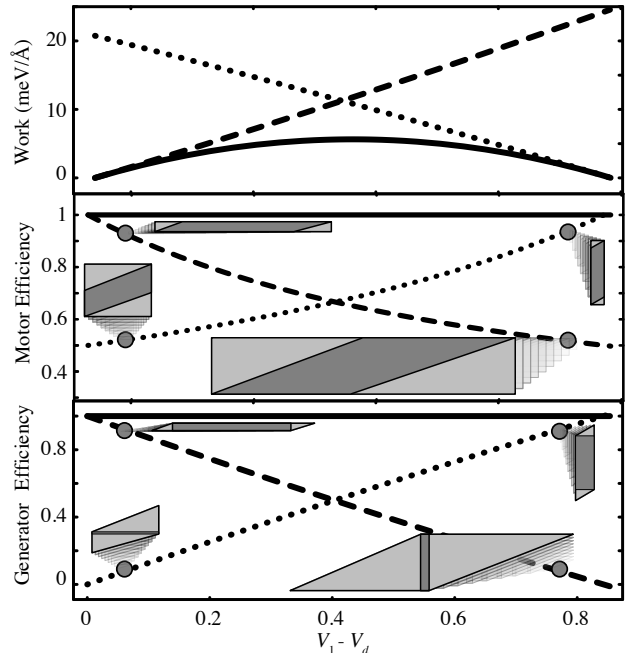


FIG. 2: Mechanical work, engine and generator efficiency as function of the voltage swing $V_1 - V_3$, for V_3 fixed at V_d . Solid, dashed and dotted lines show qV , ℓV , and $q\ell$ cycles respectively. The shaded areas of the inset glyphs (in qV -space) depict the variable efficiencies along the curves.

tors, such as dielectric elastomers²⁰, which can be fabricated in quasi-one-dimensional geometries. Writing the vibrational entropies per unit length of collapsed and inflated states as S_- and S_o , the system transitions between the two states¹² at $T_c = \frac{E_o - E_-}{S_o - S_-}$. This thermoelectromechanical coupling can be exploited to generate electrocaloric effects. These effects require tubes of sufficiently large diameter. Introduction of sulfur during synthesis can facilitate production of larger-diameter single-walled tubes²¹, and large-diameter single layers can be extracted mechanically from wide multiwalled tubes²². Multiwalled tubes themselves could also show similar deformational response, with appropriate adjustment of the effective bending modulus and electrostatic screening. We thank Paul Lammert for valuable discussions and acknowledge NSF CMMI-0727890 and DMR-0707332 for support.

¹ A. M. Fennimore, T. D. Yuzvinsky, W. Han, M. S. Fuhrer, J. Cumings, and A. Zettl, *Nature* **424**, 408 (2003).

² S. W. D. Bailey, I. Amanatidis, and C. J. Lambert, *Phys. Rev. Lett.* **100**, 256802 (2008)

- ³ H. L. Tierney, C. J. Murphy, A. D. Jewell, A. E. Baber, E. V. Iski, H. Y. Khodaverdian, A. F. McGuire, N. Klebanov, and E. C. H. Sykes, *Nature Nanotechnology*, **6**, 625 (2011)
- ⁴ F. Arico, J. D. Badjic, S. J. Cantrill, A. H. Flood, K. C.-F. Leung, Y. Liu, and J. F. Stoddart, *Topics in Current Chemistry* **249** 203 (2005)
- ⁵ N. G. Chopra, L. X. Benedict, V. H. Crespi, M. L. Cohen, S. G. Louie, and A. Zettl, *Nature* **377**, 135 (1995).
- ⁶ L. X. Benedict, V. H. Crespi, N. G. Chopra, A. Zettl, M. L. Cohen, and S. G. Louie, *Chem. Phys. Lett.* **286**, 490 (1998).
- ⁷ G. Gao, T. Cagin, and W. A. Goddard, *Nanotechnology* **9**, 184 (1998).
- ⁸ T. Tang, A. Jagota, C.-Y. Hui, and N. J. Glassmaker, *J. Appl. Phys.* **97**, 074310 (2005).
- ⁹ S. Zhang, R. Khare, T. Belytschko, K. J. Hsia, S. L. Mielke, and G. C. Schatz, *Phys. Rev. B* **73**, 075423 (2006).
- ¹⁰ E. Mockensturm and A. Mahdavi, V. Crespi, *Proc. of IMECE 2005*, 82991 (2005).
- ¹¹ O. E. Shklyae, E. Mockensturm, and V. H. Crespi, *Phys. Rev. Lett.* **106**, 155501 (2011).
- ¹² Thermal effects can also induce motion of the transition region: T. Chang and Z. Guo, *Nano Lett.* **10**, 3490 (2010).
- ¹³ L. X. Benedict, N. G. Chopra, M. L. Cohen, A. Zettl, S. G. Louie, and V. H. Crespi, *Chem. Phys. Lett.* **286**, 490 (1998).
- ¹⁴ A. Kutana and K. P. Giapis, *Phys. Rev. Lett.* **97**, 245501 (2006).
- ¹⁵ To calculate energies (including Tersoff-Brenner and Lennard-Jones contributions) per unit of length of the inflated and collapsed configurations, we constructed one periodic unit cell for each case and relaxed it at zero temperature using LAMMPS¹⁶. Following¹¹, we calculated charge and capacitance per unit length in the inflated and collapsed regions of the tube (for a screening parameter $k_s = 0.02 \text{ \AA}^{-1}$). Within our simplified model, V_d is 4.53, 8.10, 9.84 V and $\gamma = C_o/C_-$ is 1.18, 1.21, 1.24 for (40,40), (45,45), (50,50) tubes respectively.
- ¹⁶ S. Plimpton, *J. Comp Phys*, **117**, 1-19 (1995) (<http://lammps.sandia.gov>).
- ¹⁷ A transition region speed of several hundred meters per second enables a one micron long carbomorph operate at roughly 1 GHz; B. I. Yakobson, C. J. Brabec, and J. Bernholc, *J. Comput.-Aided Mater. Des.* **3**, 173 (1996); T. Chang, *Phys. Rev. Lett.* **101**, 175501 (2008).
- ¹⁸ See Supplemental Material at [URL inserted by publisher].
- ¹⁹ P. E. Lammert, P. Zhang, and V. H. Crespi, *Phys. Rev. Lett.* **84**, 2453 (2000).
- ²⁰ S. J. A. Koh, X. Zhao, and Z. Suo, *Appl. Phys. Lett.* **94**, 262902, (2009).
- ²¹ C.-H. Kiang, W. A. Goddard III, R. Beyers, and D. S. Bethune, *Carbon*, **33**, 903 (1995).
- ²² J. Cumings and A. Zettl, *Science*, **289**, 602 (2000).